International Journal of Microwave and Wireless Technologies, 2016, 8(4/5), 741–749.
doi:10.1017/S1759078716000453

RESEARCH PAPER

Substrate-integrated waveguide filters based on mushroom-shaped resonators

CRISTIANO TOMASSONI[1], LORENZO SILVESTRI[2], MAURIZIO BOZZI[2] AND LUCA PERREGRINI[2]

This paper presents a new class of quasi-elliptic pass-band filters in substrate-integrated waveguide technology, which exhibits compact size and modular geometry. These filters are based on mushroom-shaped metallic resonators, and they can be easily implemented using a standard dual-layer printed circuit board manufacturing process. The presented filters exploit non-resonating modes to obtain coupling between non-adjacent nodes in the case of in-line geometry. The resulting structure is very compact and capable of transmission zeros. In this work, the singlet configuration is preliminarily investigated, and a parametric study is performed. The design of three-pole, four-pole, and higher-order filters is illustrated with examples and thoroughly discussed. A four-pole filter operating at the frequency of 4 GHz has been manufactured and experimentally verified, to validate the proposed technique.

Keywords: New and emerging technologies and materials, Filters

Received 16 November 2015; Revised 1 March 2016; Accepted 3 March 2016; first published online 7 April 2016

I. INTRODUCTION

The deployment of a variety of novel applications in the framework of the wireless sensor networks (WSN) [1–3] and Internet of Things (IoT) [4–6] demands the development of novel classes of radio frequency (RF) and microwave components and antennas, which combine easy manufacturing, simple integration, low cost, compact size, limited loss, and low weight. Both WSN and IoT are expected to lead to the deployment of an extremely large number of wireless systems, which integrate passive and active components as well as antennas in a single, compact device. From a market point of view, the possibility to easily integrate an entire wireless system by adopting a cost-effective manufacturing process represents the key factor for the success and widespread development of these new applications.

Among the available manufacturing and integration technologies for RF and microwave circuits, a good candidate able to satisfy all the aforementioned requirements is represented by the substrate-integrated waveguide (SIW) technology [7, 8]. SIW technology permits to integrate in planar form waveguide-like components, by adopting a dielectric substrate with top and bottom ground planes and rows of metal cylinders to emulate the side walls of the waveguide. The fabrication of SIW structures can be based on well-established and low-cost manufacturing techniques, such as the standard printed circuit board (PCB) technology. SIW structures guarantee large design flexibility and easy manufacturing, combined with relatively low losses and self-packaging. Moreover, SIW allows the simple integration with active and non-linear devices, as well as the implementation of complete circuits on a single substrate, according to the system-on-substrate (SoS) paradigm [9].

Microwave filters represent a class of components very suitable for implementation in SIW technology. The main reason is related to the low losses of SIW structures, which are usually smaller than in other planar technologies (as the microstrip line or the coplanar waveguide): due to this feature, SIW filters guarantee higher quality factor. Moreover, the flexibility of SIW technology can be fully exploited in the design of filters, leading to the implementation of filters with arbitrary geometry and multilayer topology.

Several filter topologies have been proposed in SIW technology, ranging from simple inductive-post filters and filters with iris windows [10], to more complex cavity filters with circular and rectangular cavities, that permit a better design flexibility and exhibit higher selectivity, thanks to the cross-coupling that introduces transmission zeros [11]. Multilayer structures were adopted to design elliptic filters [12], and super-wide band-pass filters were developed thanks to the use of an electromagnetic band-gap structure in the ground plane [13]. A comprehensive overview of SIW filters can be found in [14–16].

A novel class of SIW filters, using non-resonating modes and based on mushroom-shaped resonators, was preliminarily presented in [17], where a three-pole filter was designed and tested. In the last years, filters based on non-resonating modes have been successfully proposed in different configurations, for instance in combination with TM cavities [18], with resonant posts in a rectangular waveguide [19], or with high-permittivity dielectric pucks [20, 21]. The non-resonating mode is a mode that resonates far away from the filter

[1]Department of Engineering, University of Perugia, Perugia, Italy
[2]Department of Electrical, Computer and Biomedical Engineering, University of Pavia, Pavia, Italy. Phone: +39 0382 985782
Corresponding author:
M. Bozzi
Email: maurizio.bozzi@unipv.it

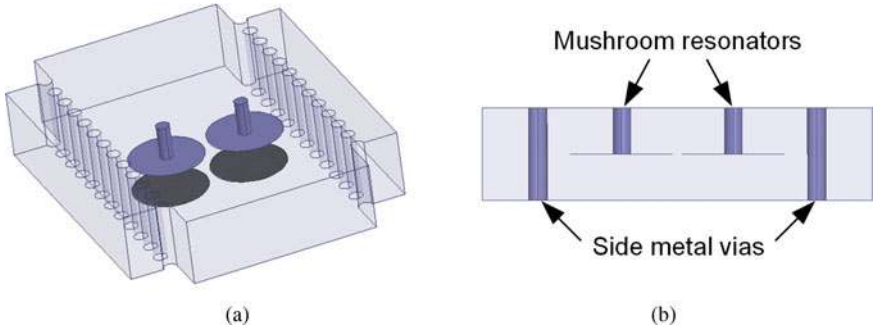

Fig. 1. Mushroom-type resonators in SIW: (a) Three-dimensional view; (b) cross-sectional view.

pass-band, and it allows for a portion of the input power to bypass the resonator, thus creating a direct source-to-load coupling able to insert transmission zeros in the filter response.

In this paper, a thorough investigation of this novel class of SIW filters is presented: in addition to the main results of the conference paper [17], a parametric investigation of the mushroom-shaped resonator is reported, as well as the design procedure for filters with an arbitrary number of poles. A four-pole filter based on mushroom-shaped resonators is designed, fabricated, and experimentally verified.

II. DUAL-MUSHROOM RESONATOR

The proposed filters are obtained by cascading dual-mushroom resonators. A dual-mushroom resonator consists of two metallic mushroom-shaped structures placed into an SIW. According to Fig. 1, each mushroom is obtained by a circular patch suspended in the SIW and connected to the broad waveguide wall by a metallic via-hole.

One of the advantages of such a structure is that it allows for quasi-elliptic filtering functions by maintaining in-line configuration. This is possible by exploiting the first two resonant modes of the dual-mushroom resonator. Figure 2 shows the electric field distribution of the first and second resonant modes, in the case of a resonator with two identical mushrooms, symmetrically placed with respect to the SIW center. The mode with lower resonant frequency has an even electric field distribution, while the other has an odd electric field distribution. This behavior can be explained considering that each mushroom is a resonator itself, and it is strongly coupled to the other mushroom, resulting in an even and odd combination of their own resonant modes.

As shown in Fig. 3, due to its even symmetry, the mode resonating at the lower frequency couples to the fundamental TE_{10} mode of the SIW, but it does not couple to the TE_{20} mode. Conversely, due to its odd symmetry, the other mode does not couple to the fundamental TE_{10} mode while it couples to the TE_{20} mode.

The basic idea is to use the odd mode of the dual-mushroom resonator to obtain the filter poles. Conversely, the even mode, which resonates far away from the filter pass-band, is used as a non-resonating mode to bypass the resonator itself and create the transmission zeros. This concept can be better explained by considering the singlet in Fig. 4(a). In this singlet configuration, source and load are represented by the SIW fundamental mode. This means that source and load are both uncoupled to the resonant mode, resulting in the frequency response of Fig. 4(b), which exhibits no filtering behavior. However, this result shows that a portion of the incident power can bypass the resonator, and this is due to the fact that the source (fundamental SIW mode) excites the non-resonating mode of the dual-mushroom resonator and, in turn, the non-resonating mode excites the load.

Figure 5 shows an asymmetric structure, with a dual-mushroom resonator consisting in mushrooms with different cup size. The field patterns of the resonating modes of this structure are slightly different from the one of the symmetric singlet with identical mushrooms. In particular, in this case, the fundamental SIW mode couples to both resonating modes as their field distribution are no longer symmetric.

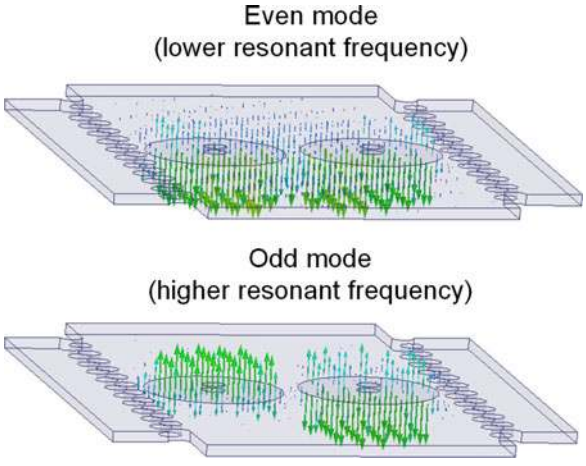

Fig. 2. Singlet composed by a dual-mushroom resonator in SIW technology: electric field distribution of the first two resonating modes.

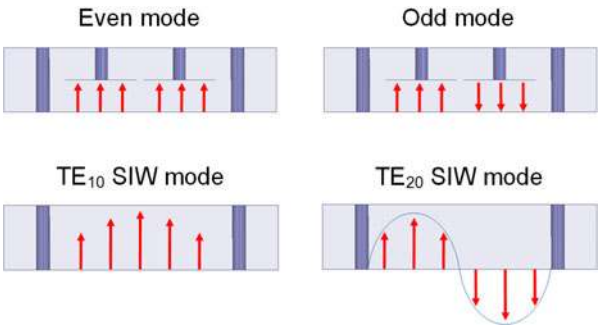

Fig. 3. Electric field pattern of the first two modes of the dual-mushroom resonator (top), and of the SIW (bottom).

https://doi.org/10.1017/S1759078716000453 Published online by Cambridge University Press

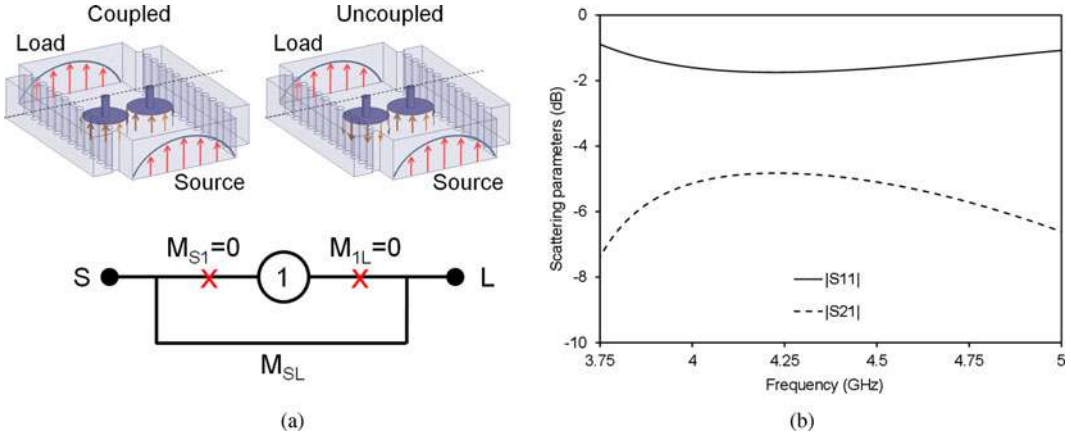

Fig. 4. Analysis of the singlet with symmetric dual-mushroom resonator: (a) geometry of the singlet and coupling scheme; (b) frequency response for the TE_{10} SIW mode.

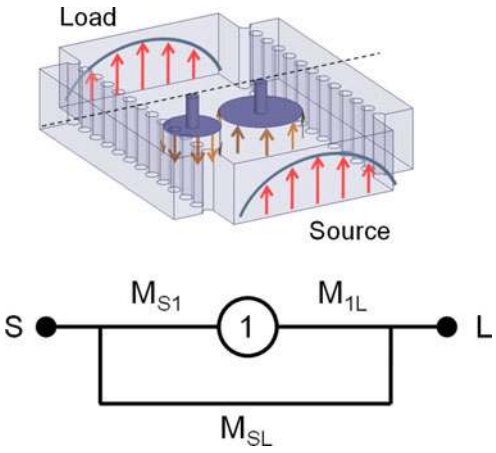

Fig. 5. Singlet with asymmetric structure, consisting in mushrooms with different cup size: geometry of the singlet and coupling scheme.

To better illustrate this phenomenon, a systematic investigation of the coupling between asymmetric singlet and fundamental SIW mode has been performed. Figure 6(a) shows a singlet where the radius of a mushroom cup is $r + dr$ and the radius the other mushroom cup is r-dr.

The frequency response for three different values of dr, while keeping r constant, is shown in Fig. 6(b)–(d), demonstrating high control capability in terms of coupling value range. As expected, the higher the value of dr, the higher the coupling of the resonant mode to source (M_{S1}) and load (M_{1L}), thus resulting in a wider filtering band. Furthermore, it is observed that all frequency responses present a transmission zero, which is due to the direct source-to-load coupling M_{SL} (Fig. 5). The presence of the transmission zero in the lower stop band depends on the fact that M_{SL} is negative and M_{S1} and M_{1L} have the same sign. Moreover, $M_{S1} = M_{1L}$, as can be easily seen by considering the symmetry of the structure along the longitudinal direction.

An out-of-band spurious can appear in the lower stop band, due to the resonant frequency of the even mode. To avoid this problem, it is convenient to use resonators with the resonance of the non-resonating mode well below the cut-off frequency of the fundamental SIW mode.

III. PARAMETRIC STUDY

In this section, a parametric study of the dual-mushroom symmetric singlet is presented. In particular, the quality factor of the resonant mode and the resonant frequency of both resonating and non-resonating modes have been analyzed.

As shown in Fig. 7, the resonator is composed by two identical mushroom structures symmetrically positioned with respect to the SIW center. The SIW dimensions are the following: center-to-center width 40 mm, post diameter 2 mm, and longitudinal spacing 3.5 mm. The relative dielectric permittivity of the substrate is 2.2, and its thickness is 1 mm. The parametric study is performed by considering the distance P_s between the center of the waveguide and the circular patch (mushroom cup), the distance S between the center of the post (mushroom stalk) and the center of the circular patch, and finally the post diameter d.

In the first analysis, the variation of the mushroom distance $2P_s$ is considered. Figure 8(a) shows that the Q factor of the resonator is practically unaffected by this parameter. In Fig. 8(b), the influence of the same parameter on resonant frequencies of the first two modes is shown. In this case, there is a small effect, and the separation between the two resonances decreases when the mushroom distance increases.

According to Fig. 8(b), for this particular structure it seems convenient to maintain the two mushrooms as close as possible. In fact, in dual-mushroom filters it is better to have a high separation between the two resonant frequencies. This is due to the fact the resonance of the non-resonating modes can generate spurious frequencies in the lower stop band.

In the second parametric analysis, the effect of the stalk not centered with the mushroom cap is considered. Figure 9(a) shows the Q factor of the resonator versus the stalks shift S: the Q factor is maximum for $S = 0$, and it decreases when the stalk is shifted toward the SIW center ($S > 0$), or toward the SIW walls ($S < 0$). Figure 9(b) shows the resonant frequency of the first two modes versus S: the mode separation increases when the two stalks become closer. Therefore, the stalk shift can be used to manage spurious frequencies in the lower stop band, if necessary, but the centered post seems the best solution.

https://doi.org/10.1017/S1759078716000453 Published online by Cambridge University Press

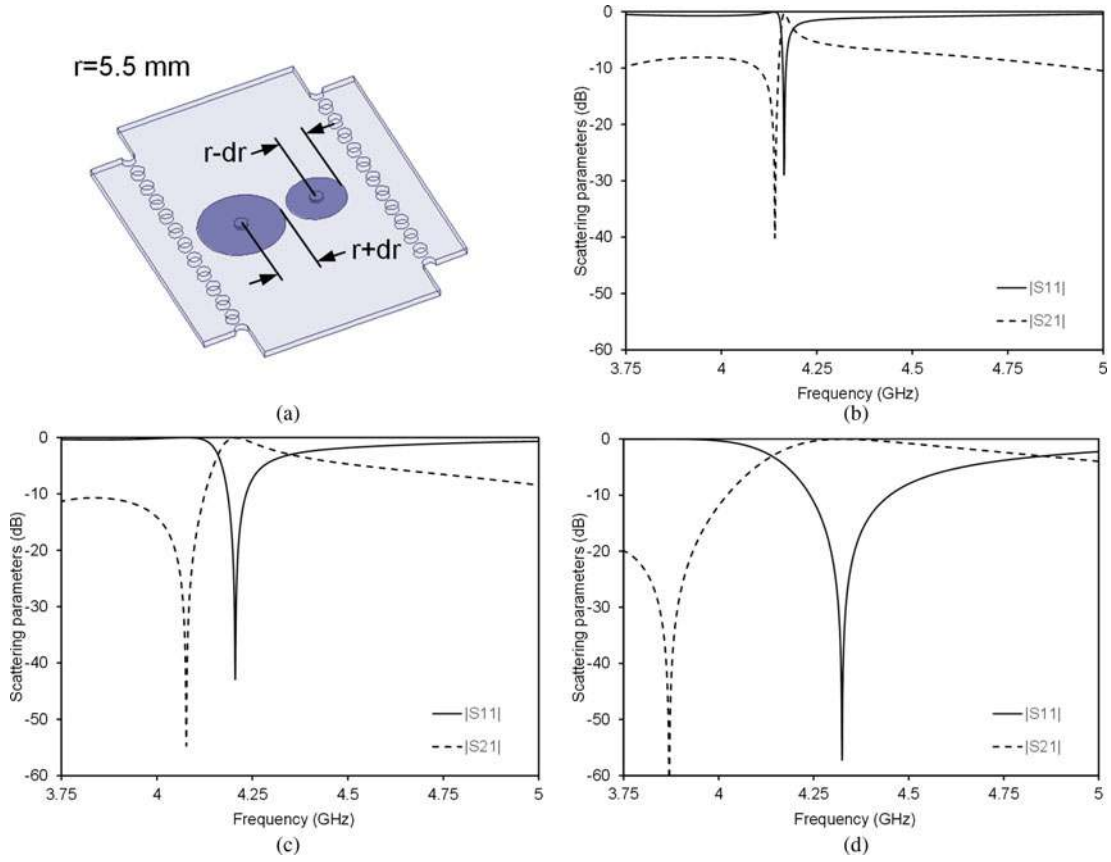

Fig. 6. Analysis of the singlet with the resonator with different cup size: (a) geometry of the singlet; (b) frequency response for $dr = 0.2$ mm; (c) frequency response for $dr = 0.5$ mm; (d) frequency response for $dr = 1$ mm.

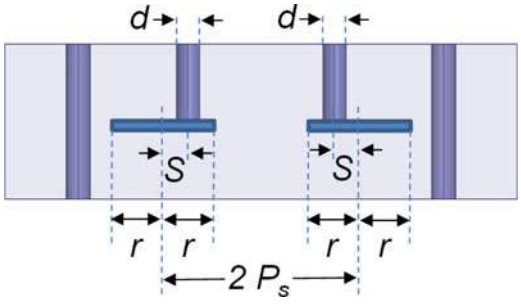

Fig. 7. Double-mushroom resonator consisting in two identical post symmetrically placed with respect to the SIW center.

The last considered parameter is the mushroom stalk diameter d. Figure 10(a) shows that the diameter d affects the Q factor, and better results are obtained for larger diameters. On the other hand, as shown in Fig. 10(b), larger diameters also allow for higher resonant frequency distance, thus resulting in a better behavior in terms of lower stop-band spurious frequencies.

IV. DESIGN OF N-TH ORDER FILTER

The N-th order filters can be obtained by cascading N resonators. In Fig. 11(a), a structure is obtained by cascading N dual-mushroom symmetric resonators, consisting of pairs of identical mushrooms symmetrically placed with respect to the SIW center. In this structure, the coupling between adjacent resonators is obtained by exploiting the TE_{20} mode of the SIW. However, this structure is not yet a filter, as the resonators are not coupled to the source and the load. This problem can be easily overcome using the structure shown in Fig. 11(b), where the first and last resonators are replaced by asymmetric resonators, consisting of pairs of different mushrooms. In fact, asymmetric resonators couple with the fundamental mode of the SIW, as discussed in Section II.

As shown in Fig. 6, the desired coupling M_{S_1} between the source and the first (asymmetric) resonator can be obtained by properly selecting the value of dr. The same procedure applies for the coupling M_{NL} between the last (asymmetric) resonator and the load. Conversely, the desired coupling between adjacent (symmetric) resonators is obtained by exploiting the attenuation of the non-propagating TE_{20} mode of the SIW: the higher the distance between two adjacent resonators, the smaller their coupling. Figure 12 reports the coupling between symmetric resonators versus their distance, in the case $r = 7.25$ mm, $d = 7$ mm. The SIW dimensions are the following: center-to-center width 40 mm, post diameter 2 mm, and longitudinal spacing 3.5 mm. The relative dielectric permittivity of the substrate is 2.2, and its thickness is 1 mm.

According to Fig. 11(b), the fundamental mode of the SIW generates additional coupling between non adjacent elements, namely: direct source-to-load coupling M_{SL},

https://doi.org/10.1017/S1759078716000453 Published online by Cambridge University Press

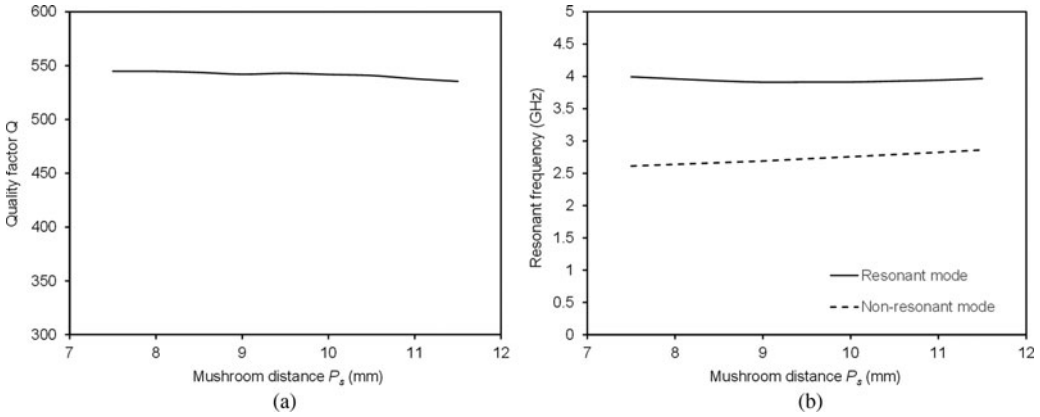

Fig. 8. Investigation of the mushroom distance P_s from the waveguide center (with $r = 7.15$ mm, $S = 0$, $d = 6.5$ mm): (a) resonator Q factor versus P_s; (b) resonant frequency of resonant and non-resonating modes versus P_s.

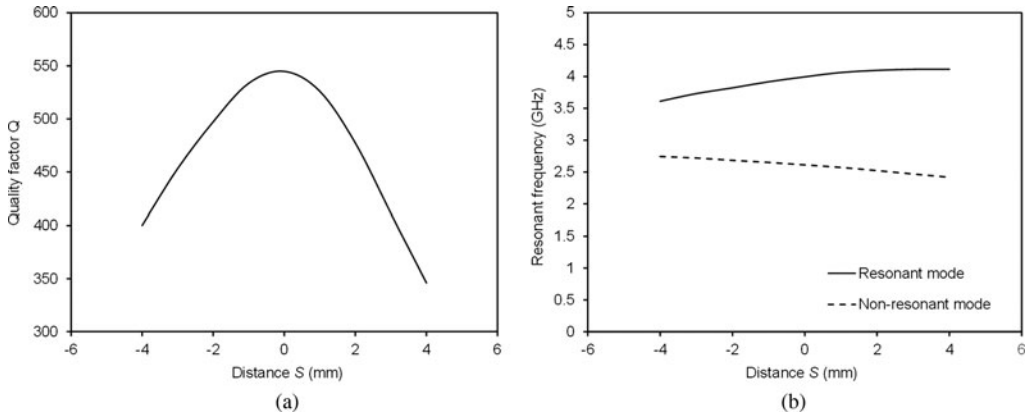

Fig. 9. Investigation of the distance S between mushroom stalk center mushroom and cup center (with $r = 7.15$ mm, $P_s = 7.5$ mm, and $d = 6.5$ mm): (a) resonator Q factor versus S; (b) resonant frequency of resonant and non-resonating modes versus S.

coupling M_{SN} between source and last resonator, coupling M_{1L} between first resonator and load, and coupling M_{1N} between first and last resonators. Such additional couplings allow for filtering function with transmission zeros.

This design procedure has been applied to the design of a third-order filter and of a fourth-order filter. In Fig. 13, the coupling patterns and the relevant coupling matrix of the third-order filter are shown. The dimensions of the filter implementing this coupling matrix are reported in Fig. 14(a), while Fig. 14(b) shows the comparison between the frequency response obtained by the full-wave analysis and the one obtained by the coupling matrix. A transmission zero due to the coupling between non-adjacent elements appears in the upper stop band, thus increasing the selectivity of the filter in the upper cutoff. In the lower stop band, a

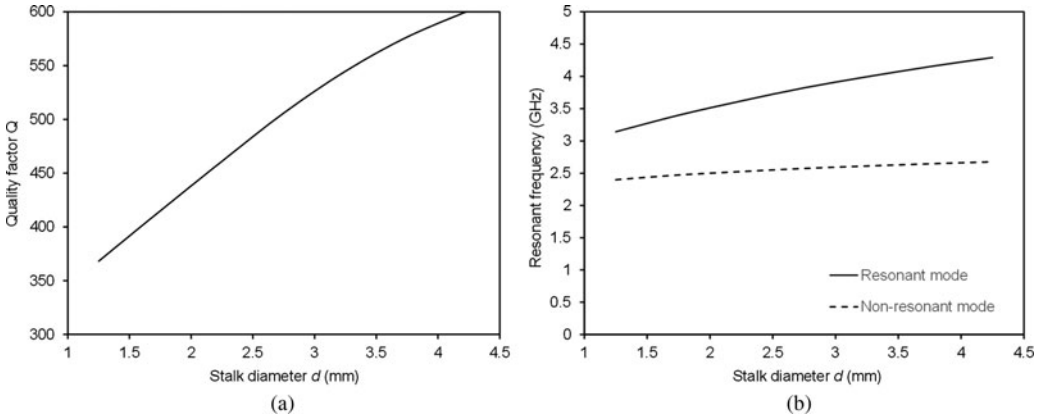

Fig. 10. Investigation of the stalk diameter d (with $r = 7.15$ mm, $P_s = 7.5$ mm and $S = 0$): (a) resonator Q factor versus d; (b) resonant frequency of resonant and non-resonating modes versus d.

https://doi.org/10.1017/S1759078716000453 Published online by Cambridge University Press

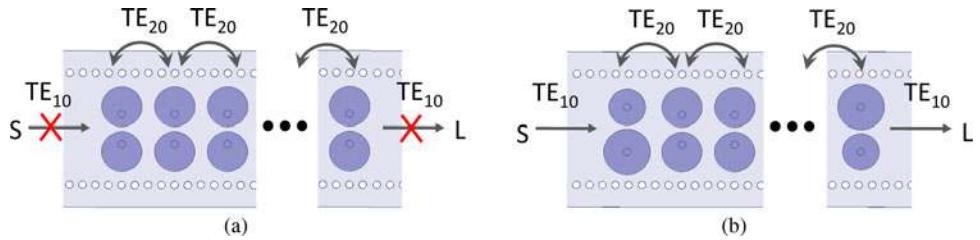

Fig. 11. Cascade of dual-mushroom resonators: (a) structure based on symmetric resonators only, which do not couple to source and load; (b) structure with first and last asymmetric resonators, which allows obtaining a filter.

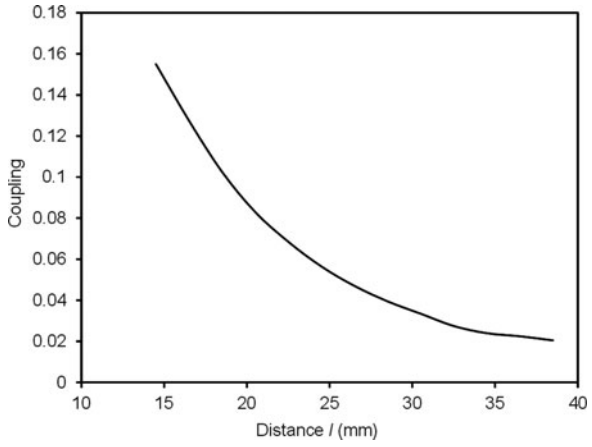

Fig. 12. Coupling between two adjacent dual-mushroom symmetric resonators as a function of their distance.

spurious frequency appears, due to the resonance of the non-resonating modes (Fig. 14(b)).

To overcome the spurious problem it is important to design the structure so as the non-resonating modes resonate well below the input/output waveguide cutoff. In the design of the fourth-order filter implementing the coupling matrix of Fig. 15, two different strategies have been combined to fulfill this result. According to Fig. 16(a), the first strategy consists in the use of input and output waveguides narrower than the waveguide containing the resonators, while the second strategy consists in the use of posts with large diameter to increase the distance between the resonant frequency of resonant and non-resonating modes (see Fig. 10(b)). The comparison between full-wave analysis of the filter and coupling matrix response is shown in Fig. 16(b). This filter has no spurious in the lower stop band. The filter response presents two transmission zeros very close to the filter band: one in the lower stop band and the other in the upper stop band, resulting in a very selective filter.

V. EXPERIMENTAL VALIDATION

The SIW filters described in Section IV have been manufactured and measured, to validate the proposed filter topology. The experimental verification of the three-pole filter shown in Fig. 14 has been reported in [17], whereas the fabrication and measurement of the four-pole filter shown in Fig. 16 is discussed in this section.

The four-pole filter has been implemented by adopting two layers of Taconic TLY-5–200, with dielectric thickness $h = 0.508$ mm, metal thickness $t = 35$ μm, relative dielectric permittivity $\varepsilon_r = 2.2$, and loss tangent $\tan\delta = 0.0009$. The filter was manufactured using a LPKF milling machine, and the two dielectric layers were attached using TacBond bonding film (with thickness 38 μm and relative dielectric permittivity 2.35). The metal vias have been metalized using a conductive paste.

The photograph of the filter prototype before assembly is shown in Fig. 17: it displays the top side of the top layer, including the transition from SIW to microstrip lines, and the top side of the bottom layer, with the circular metal patches forming the mushroom resonators.

Figure 18 shows the simulated and measured frequency response of the four-pole filter, in the frequency band from 2 to 6 GHz. The measured band-pass frequency exhibits a shift of 100 MHz with respect to the simulation results, and a measured insertion loss of 2.47 dB (including connectors, microstrip lines, and transitions). The first upper spurious band appears at 5.8 GHz, and the out-of-band rejection is better than 25 dB from 4.15 to 5.75 GHz.

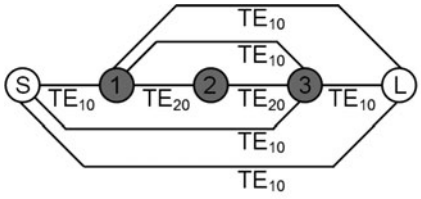

	S	1	2	3	L
S	0	1.0423	0	-0.0905	-0.0399
1	1.0423	0	0.9652	0.1505	0.0905
2	0	0.9652	-0.2568	0.9652	0
3	-0.0905	0.1505	0.9652	0	-1.0423
L	-0.039	0.0905	0	-1.0423	0

(b)

Fig. 13. Topology of the three-pole filter: (a) coupling routing scheme for the filter (with indication of the mode responsible for the coupling); (b) relevant coupling matrix.

https://doi.org/10.1017/S1759078716000453 Published online by Cambridge University Press

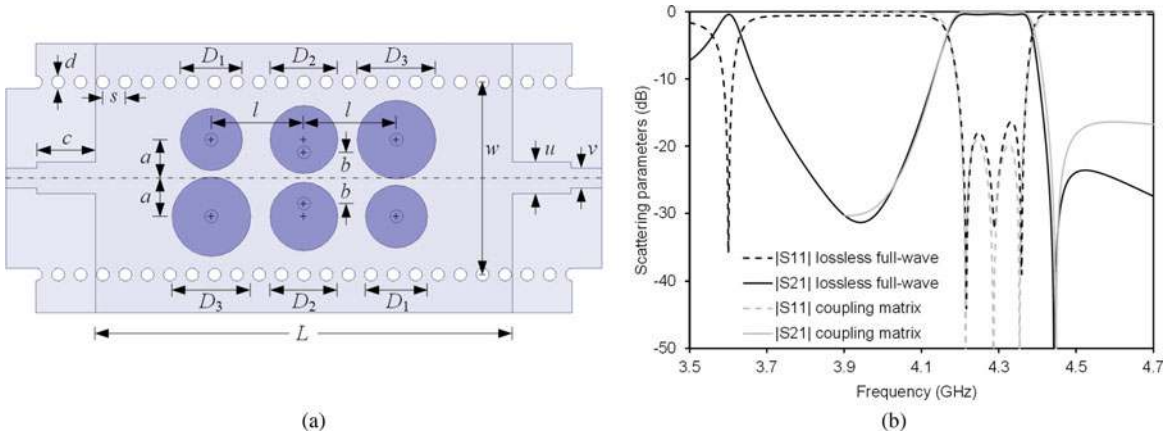

Fig. 14. Design of the three-pole filter: (a) drawing of the filter (dimensions in mm: $a = 6$, $b = 4$, $c = 9.2$, $d = 2$, $s = 3.5$, $w = 30$, $u = 5$, $v = 3.1$, $l = 14.5$, $L = 65.3$, $D_1 = 9.7$, $D_2 = 10.61$, $D_3 = 12.3$); (b) frequency response of the filter (comparison between full-wave response by Ansys HFSS and the coupling matrix response).

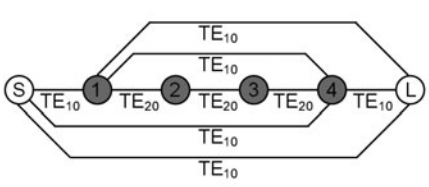

	S	1	2	3	4	L
S	0	0.9988	0	0	-0.0118	0.0368
1	0.9988	0	0.8314	0	-0.163	0.0118
2	0	0.8314	0	0.7602	0	0
3	0	0	0.7602	0	0.8314	0
4	-0.0118	-0.163	0	0.8314	0	-0.9988
L	0.0368	0.0118	0	0	-0.9988	0

(b)

Fig. 15. Topology of the four-pole filter: (a) coupling routing scheme for the filter (with indication of the mode responsible for the coupling); (b) relevant coupling matrix.

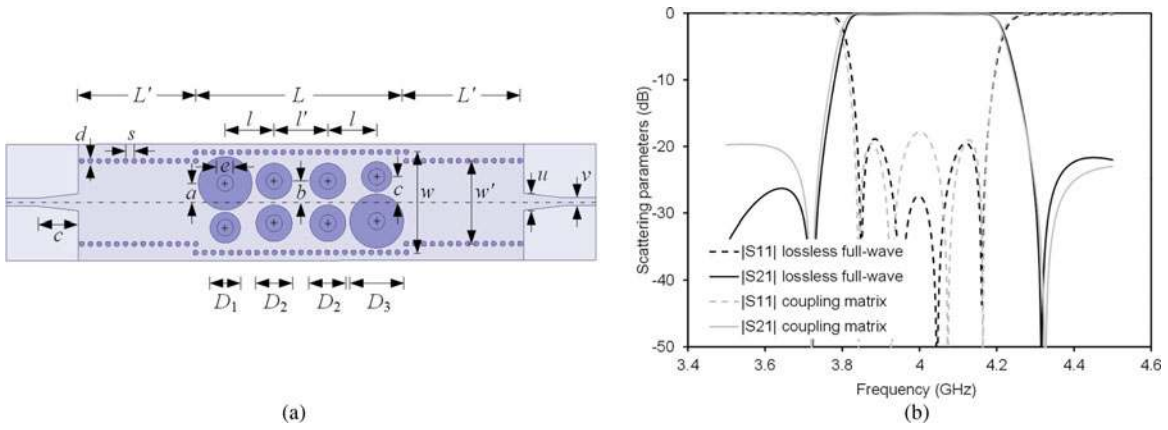

Fig. 16. Design of the four-pole filter: (a) drawing of the filter (dimensions in mm: $L' = 45.5$, $L = 84$, $l = 19.5$, $l' = 21.45$, $d = 2$, $s = 3.5$, $e = 6.5$, $a = 7.53$, $b = 8.38$, $c = 10.13$, $w = 40$, $w' = 33$, $u = 6.89$, $v = 3.1$, $c = 16$, $D_1 = 12.09$, $D_2 = 14.36$, $D_3 = 21.45$); (b) frequency response of the filter (comparison between full-wave response by Ansys HFSS and the coupling matrix response).

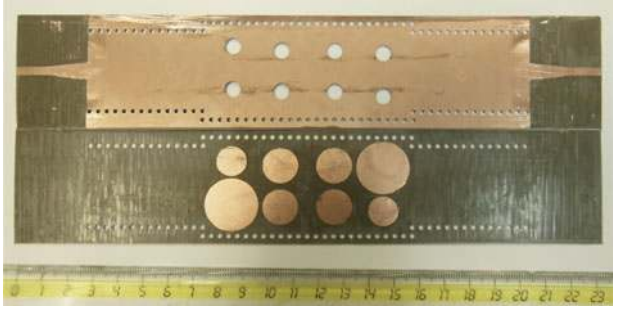

Fig. 17. Photograph of the four-pole filter: top side of the top layer and top side of the bottom layer.

VI. CONCLUSION

This paper has presented a novel class of SIW filters, based on the use of mushroom-shaped resonators. The use of non-resonating modes allows us to achieve compact inline filters with transmission zeros in the frequency response. The coupling mechanisms between symmetric/asymmetric pairs of mushroom resonators and the first two modes of the SIW have been investigated in detail, and the design strategy for filters with arbitrary number of poles has been presented. Filters with three and four poles have been designed by adopting the proposed

https://doi.org/10.1017/S1759078716000453 Published online by Cambridge University Press

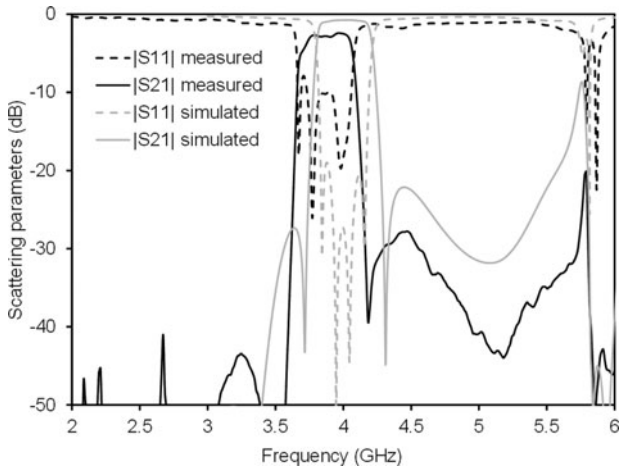

Fig. 18. Frequency response of the four-pole filter: simulation results from Ansys HFSS are compared to measured data.

technique, and the experimental verification of the four-pole filter has been reported.

REFERENCES

[1] Akyildiz, I.F.; Vuran, M.C.: Wireless Sensor Networks, John Wiley & Sons, Chichester, UK, 2010.

[2] Dargie, W.; Poellabauer, C.: Fundamentals of Wireless Sensor Networks: Theory and Practice, John Wiley & Sons, Chichester, UK, 2010.

[3] Yang, S.-H.: Wireless Sensor Networks: Principles, Design and Applications, Springer, London, 2014.

[4] Giusto, D.; Iera, A.; Morabito, G.; Atzori, L. (Eds.): The Internet of Things, Springer, London, 2010.

[5] Special Issue: The Internet of Things. IEEE Wireless Communications, 6 (2010).

[6] Special Issue: The Internet of Things', IEEE Communications Magazine, 11 (2011).

[7] Bozzi, M.; Georgiadis, A.; Wu, K.: Review of substrate integrated waveguide (SIW) circuits and antennas. IET Microw. Antennas Propag., **5** (2011), 909–920.

[8] Garg, R.; Bahl, I.; Bozzi, M.: Microstrip Lines and Slotlines, 3rd ed., Artech House, Boston/London, 2013.

[9] Wu, K.: Towards system-on-substrate approach for future millimeter-wave and photonic wireless applications, in Asia-Pacific Microwave Conf., 2006.

[10] Deslandes, D.; Wu, K.: Single-substrate integration technique of planar circuits and waveguide filters. IEEE Trans. Microw. Theory Tech., **51** (2003), 593–596.

[11] Chen, X.-P.; Wu, K.: Substrate integrated waveguide cross-coupled filter with negative coupling structure. IEEE Trans. Microw. Theory Tech., **56** (2008), 142–149.

[12] Hao, Z.C.; Hong, W.; Chen, X.P.; Chen, J.X.; Wu, K.; Cui, T.J.: Multilayered substrate integrated waveguide (MSIW) elliptic filter. IEEE Microw. Wireless Compon. Lett., **15** (2005), 95–97.

[13] Hao, Z.-C.; Hong, W.; Chen, J.-X.; Chen, X.-P.; Wu, K.: Compact super-wide bandpass substrate integrated waveguide (SIW) filters. IEEE Trans. Microw. Theory Tech., **53** (2005), 2968–2977.

[14] Chen, X.-P.; Wu, K.: Substrate integrated waveguide filter: basic design rules and fundamental structure features. IEEE Microw. Mag., **15** (2014), 108–116.

[15] Chen, X.-P.; Wu, K.: Substrate integrated waveguide filters: design techniques and structure innovations. IEEE Microw. Mag., **15** (2014), 121–133.

[16] Chen, X.-P.; Wu, K.: Substrate integrated waveguide filters: practical aspects and design considerations. IEEE Microw. Mag., **15** (2014), 75–83.

[17] Tomassoni, C.; Silvestri, L.; Bozzi, M.; Perregrini, L.: Quasi-elliptic SIW band-pass filter based on mushroom-shaped resonators, in 45th European Microwave Conf., Paris, France, 2015.

[18] Tomassoni, C.; Bastioli, S.; Sorrentino, R.: Generalized TM dual-mode cavity filters. IEEE Trans. Microw. Theory Tech., **59** (2011), 3338–3346.

[19] Tomassoni, C.; Sorrentino, R.: A new class of pseudoelliptic waveguide filters using dual-post resonators. IEEE Trans. Microw. Theory Tech., **61** (2013), 2332–2339.

[20] Pelliccia, L.; Cacciamani, F.; Tomassoni, C.; Sorrentino, R.: Ultra-compact high-performance filters based on TM dual-mode dielectric-loaded cavities. Int. J. Microw. Wireless Technol., **6** (2014), 151–159.

[21] Bastioli, S.; Snyder, R.S.: Inline pseudoelliptic $TE_{01\delta}$ mode dielectric resonator filters using multiple evanescent modes to selectively bypass orthogonal resonators. IEEE Trans. Microw. Theory Tech., **60** (2012), 3988–4001.

Cristiano Tomassoni was born in Spoleto, Italy. He received the Laurea degree and Ph.D. degree in Electronics Engineering from the University of Perugia, Perugia, Italy, in 1996 and 1999, respectively. In 1999, he was a Visiting Scientist with the Lehrstuhl für Hochfrequenztechnik, Technical University of Munich, Munich, Germany. From 2000 to 2007, he was a Postdoctoral Research Associate with the University of Perugia. In 2001, he was a Guest Professor with the Fakultät für Elektrotechnik und Informationstechnik, Otto-von-Guericke University, Magdeburg, Germany. Since 2007, he has been an Assistant Professor with the University of Perugia. His main area of research concerns the modeling and design of waveguide devices and antennas. His research interests also include the development of reduced-size cavity filters, reconfigurable filters, and printed reconfigurable antenna arrays. Dr. Tomassoni was the recipient of the 2012 Microwave Prize presented by the IEEE Microwave Theory and Technique Society (IEEE MTT-S).

Lorenzo Silvestri was born in Novara, Italy, in 1987. He received the Master degree in Electronic Engineering in 2014 from the University of Pavia. He is currently working as a post-graduate scholar at the Department of Industrial and Information Technology (University of Pavia). His main interests are related to the development of new components in substrate-integrated waveguide (SIW) technology on innovative substrate materials.

https://doi.org/10.1017/S1759078716000453 Published online by Cambridge University Press

Maurizio Bozzi received the Ph.D. degree in Electronics and Computer Science from the University of Pavia in 2000. He held research positions with various universities, including the Technische Universität Darmstadt, Germany, the Universitat de Valencia, Spain, and the École Polytechnique de Montréal, Canada. In 2002, he joined the University of Pavia, where he is currently an Associate Professor. He is also a Guest Professor of the Tianjin University, China. His main research interests concern the development of numerical methods for the electromagnetic modeling and design of microwave components. He authored or co-authored more than 88 journal papers and 230 conference papers, and the book Microstrip Lines and Slotlines (Artech House, 2013). Professor Bozzi was the General Chair of IEEE NEMO2014 Conference and IEEE MTT-S IMWS2011 Conference. He is an Associate Editor for IEEE Microwave and Wireless Components Letters, IET Microwaves, Antennas & Propagation, and Electronics Letters, and a member of the General Assembly of the European Microwave Association (2014–2016). He received several awards, including the 2014 Premium Award for Best Paper in Electronics Letters and the 2015 Premium Award for Best Paper in IET Microwaves, Antennas & Propagation.

Luca Perregrini received the Laurea degree in Electronics (1989) and the Ph.D. degree in Electronics (1993) from the University of Pavia, Italy. In 1992, he joined the Department of Electronics of the University of Pavia, Italy, where he is now an Associate Professor of electromagnetics. His main research interests are in numerical methods for electromagnetics, design of passive components and periodic structures, large reflector antennas, and industrial application of microwaves. He has authored or co-authored more than 82 journal, 230 conference papers, six book chapters, and two textbooks. He was the co-editor of the book Periodic Structures (Research Signpost, 2006). He is an associate editor of *IEEE Transactions on Microwave Theory and Techniques, International Journal of Microwave and Wireless Technologies*, and *Electronic Letters*. He has been an associate editor of the *IEEE Microwave and Wireless Components Letters* (2010–2013), a member of the General Assembly of the European Microwave Association (2011–2013), TPC Chair of EuMC2014 and of IEEE NEMO2014, and member of the TPC of several conferences. He is a Fellow of IEEE.

https://doi.org/10.1017/S1759078716000453 Published online by Cambridge University Press